Supplemental Data

A. MATERIALS AND METHODS

B. SUPPORTING TABLES

1. **Table S1.** Samples and their tagged primers used for amplifying 16S rRNA genes
2. **Table S2.** Summary of numbers of sequences and OTUs, and Shannon index for each sample at aCO_2 or eCO_2 based on pyrosequencing data
3. **Table S3.** The classified phylotypes detected at different taxonomical levels
4. **Table S4.** Statistical analysis of differences in the microbial community composition and structure between aCO_2 and eCO_2 at the community and phylum levels
5. **Table S5.** Numbers of shared OTUs that were significantly ($p < 0.05$) changed at eCO_2 based on the scaled abundances and unique OTUs detected only at aCO_2 or eCO_2
6. **Table S6.** Partial Mantel analysis of the relationship between the relative abundance of phylum and soil or plant properties
7. **Table S7.** Partial Mantel analysis of the relationship between the relative abundance of order and soil or plant properties
8. **Table S8.** Partial Mantel analysis of the relationship between the relative abundance of family and soil or plant properties
9. **Table S9.** Partial Mantel analysis of the relationship between the relative abundance of genus and soil or plant properties

C. SUPPORTING FIGURES

1. **Fig. S1.** Neighbor-Joining tree of representative sequences of 16S rRNA genes major phyla detected at aCO_2 and eCO_2. Different phyla are presented by different colors on the circle tree.

2. **Fig. S2.** Significantly changed OTUs in the phylum of Actinobacteria at elevated CO_2 using the response ratio method (47) at 95% confidence interval.
3. **Fig. S3.** Significantly changed microbial populations at the order levels in the phylum of Proteobacteria.
4. **Fig. S4.** Significantly changed microbial populations at the class or lower levels in the phylum of Acidobacteria (A), Verrucomicrobia (B), and Firmicutes (C).
5. **Fig. S5.** The flowchart of OTU identification processes.

D. SUPPLEMENTAL REFERENCES

A. MATERIALS AND METHODS

1.1. Site and sampling

The artificially elevated CO_2 field site is located at the Cedar Creek Ecosystem Science Reserve in Minnesota, USA (lat. 45 ° N, Long. 93 ° W), which is also named as BioCON (Biodiversity, CO_2 and N). It has been established on a secondary successional grassland of a sandy outwash soil after removing the previous vegetation since 1997 (53). Totally, 296 plots (2 x 2 m) are evenly distributed in six 20-meter diameter rings. Three of them are exposed to an ambient CO_2 concentration of 368 ppm, and other three are under an elevated CO_2 concentration of 560 ppm by using a free-air CO_2 enrichment (FACE) system (46). Four levels of plant diversity: 1, 4, 9, or 16 species were randomly planted for each plot with 32, 15, 15 and 12 replicates, respectively. Half of those plots, selected at random, receive the equivalent of 4 g N (NH_4NO_3) m^{-2} $year^{-1}$. In this study, a total of 24 plots including 12 from ambient CO_2 and 12 from elevated CO_2, and all have 16 plant species but without additional N supply. A series of measurements were routinely performed, including (i) plants (including aboveground and belowground biomass, plant C and N, and the C/N ratio), and (ii) soil physical (volumetric moisture and pH), chemical (soil C and N) properties, and biological processes (net N mineralization and nitrification rates).

Soil samples were taken in July, 2007 under ambient and elevated CO_2 conditions for microbial community analyses. Each sample was composited from five soil cores at a depth of 0-15 cm. All samples were immediately transported to the laboratory where they were immediately frozen and stored at -80^{o}C.

1.2. Plant species, functional groups and biomass measurements

The 16 perennial species used in this study were all native or naturalized to the Cedar Creek Ecosystem Science Reserve, and they are in four functional groups: (i) four C3 grasses (*Agropyron repens*, *Bromus inermis*, *Koeleria cristata*, *Poa pratensis*), (ii) four C4 grasses (*Andropogon gerardii*, *Bouteloua gracilis*, *Schizachyrium scoparium*, *Sorghastrum nutans*), (iii) four N-fixing legumes (*Amorpha canescens*, *Lespedeza capitata*, *Lupinus perennis*, *Petalostemum villosum*), and (iv) four non N-fixing herbaceous species (*Achillea millefolium*, *Anemone cylindrica*, *Asclepias tuberosa*, *Solidago rigida*). Plots were regularly weeded to remove unwanted species, though the 16 species plots used in this study require minimal weeding. Plant species hereafter are referred to by their genus, and the four functional groups of plants are referred to as C3, C4, legume and forb (53).

The aboveground and belowground (0–20 cm) biomass and plant C and N concentrations were measured (52, 53). A 10 x 100 cm strip was clipped at just above the soil surface, and all plant material was collected, sorted to live material and senesced litter, dried and weighed. Roots were sampled at 0–20 cm depth using three 5-cm diameter cores in the area used for the aboveground biomass clipping. Roots were washed, sorted into fine (< 1 mm diameter) and coarse classes and crowns, dried and weighed. A composite sample was taken from aboveground and belowground biomass from each plot from the August harvest of each year, ground and analyzed for N using a Costech ECS 4010 element analyzer (Costech Analytical Technologies, Inc., Valencia, CA).

1.3. Soil physical, chemical, and biological properties

Soil physical properties. Soil pH and volumetric soil moisture were measured at different depths of 0-17, 42-59, and 83-100 cm in a KCl slurry and with permanently placed TRIME Time Domain Reflectometry (TDR) probes (Mesa Systems Co., Medfield MA), respectively.

Soil chemical properties. Total soil C and N were measured at depths of 0-10, 10-20, 20-40 and 40-60 cm for each plot on a Costech ECS 4010 element analyzer (Costech Analytical Technologies, Inc., Valencia, CA).

Net N mineralization. Net N mineralization rates were measured concurrently in each plot for one-month *in situ* incubations with a semi-open core at 0-20 cm depth during the mid summer of each year (52, 53). Net N mineralization rates were determined by the difference between the final and initial NH_4^+-N + NO_3^--N pool sizes determined with 1 M KCl extractions. Net nitrification was determined by the difference between the final and initial NO_3^--N pool sizes.

1.4. DNA extraction, purification and quantitation

Soil DNA was extracted by freeze-grinding mechanical lysis (58), and was purified using a low melting agarose gel followed by phenol extraction. DNA quality was assessed by the ratios of 260/280 nm, and 260/230 nm using a NanoDrop ND-1000 Spectrophotometer (NanoDrop Technologies Inc., Wilmington, DE), and final soil DNA concentrations were quantified with PicoGreen (29) using a FLUOstar Optima (BMG Labtech, Jena, Germany).

1.5. 454 pyrosequencing analysis

1.5.1. Sample tagging and PCR amplicon preparations. Based on the V4-V5 hypervariable regions of bacterial 16S rRNAs (*Escherichia coli* positions 515-907), the univer*sal PCR primers,* F515: GTGCCAGCMGCCGCGG and R907: CCGTCAATTCMTTTRAGTTT were selected.

Both primers were then checked with the ribosomal database due to July 2007 (37), and covered > 95% of the 16S gene sequences in the database. To pool multiple samples for one run of 454 sequencing, a sample tagging approach was adopted (31, 42). In this study, a unique 6-mer tag for each of 24 DNA samples was added to the 5'-end of both primers, and those tag-primers were synthesized by Invitrogen (Carlsbad, CA) and used for the generation of PCR amplicons. The amplification mix contained 10 units of Pfu polymerase (BioVision, Mountain View, CA), 5 µl Pfu reaction buffer, 200 µM dNTPs (Amersham, Piscataway, NJ), and a 0.2 µM concentration of each primer in a volume of 50 µl. Genomic DNA (10 ng) was added to each amplification mix. Cycling conditions were an initial denaturation at 94℃ for 3 min, 30 cycles of 95℃ 30 s, 58℃ for 60 s, and 72℃ for 60 s, a final 2-min extension at 72℃. Normally, multiple (5-10) 50 µl reactions were needed for each sample, and the products were pooled together after amplification and purified by agarose gel electrophoresis. The amplified PCR products were recovered and then quantitated with a PicoGreen method using a FLUOstar Optima (BMG Labtech, Jena, Germany). Finally, amplicons of all samples were pooled in an equimolar concentration for 454 pyro-sequencing.

1.5.2. 454 pyrosequencing. The fragments in the amplicon libraries were repaired and ligated to the 454 sequencing adapters, and the resulting products were bound to beads under conditions that favor one fragment per bead. The beads were emulsified in a PCR mixture in oil, and PCR amplification occurred in each droplet, generating millions of copies of a unique DNA template. After breaking the emulsion, the DNA strands were denatured, and beads carrying single-stranded DNA clones were deposited into wells on a PicoTiter-Plate (454 Life Sciences) for pyrosequencing (48) on a FLX 454 system (454 Life Sciences, Branford, CT). For this study, we recovered 92,120 sequence reads that represented both forward and reverse reads of 24 samples

with an average length around 230 bp. All pyrosequencing reads were initially processed using the RDP pyrosequencing pipeline (http://pyro.cme.msu.edu/pyro/index.jsp) (37).

1.5.3. Assignment of sequence reads to samples. The raw sequences were sorted and distinguished by unique sample tags. Since each sample had a unique tag, all sequence reads with the same tag were assigned to the same sample. Also according to the primer sequences, each sample could be further separated into two (forward and reverse) regions. Finally, the tag and both primers were trimmed. For all 24 samples, the number of reads ranged from 2509 to 5152.

1.5.4. Removal of low-quality sequences. To minimize effects of random sequencing errors, we eliminated (*i*) sequences that did not perfectly match the PCR primer at the beginning of a read, (*ii*) sequences with non-assigned tags, (*iii*) sequence reads with < 150 *bp* after the proximal PCR primer if they terminated before reaching the distal primer, and (*iv*) sequences that contained more than one anonymous nucleotide (N). Finally, a total of 77,653 sequences remained with an average length of 251 bases. There were 35,289 reads derived from the forward region and 42,355 reads derived from the reverse region. All these sequences can be downloaded at http://ieg.ou.edu/4download/.

1.5.5. Classification of 454 sequences and OTUs assignment. Since the average length of PCR amplicons produced from this used primer pair is 390 bases, it is expected that there was an approximately150-base overlap between the forward and reverse regions if an amplicon was from the same molecule. To address this issue, we develop a flowchart to classify all sequences into OTUs (Fig. S1). Two major steps were performed: (i) independent OTU identification for either forward or reverse region, and (ii) a combination of forward and reverse OTUs identified in (i). First, for independent OTU identification, all forward or reverse sequences from 24

samples were pooled together, independently aligned by a RDP Infernal Aligner (50), and then classified into OTUs within a 0.03 difference (55), resulting in two (forward and reverse) sets of OTUs. Second, all sequences from both regions of each tag were performed BLASTN against each other. If two reads from the forward and reverse parts had an overlap region, which had 100% identity and was more than 100-base long, these two reads were considered from the same molecule, and then combined as a single sequence. Thereafter, if reads from a forward OTU and a reverse OTU had one or multiple overlapped regions, all reads of these OTUs were pooled together and formed a new OTU, and OTUs whose reads had no overlaps in forward and reverse regions were kept unaffected (56). Any singleton OTUs (with only one read) were removed and all other remained sequences from forward, reverse and combined OTUs were sorted into each sample based on OTUs. Finally, all sequences were gone through QIIME (33) chimera check program and all potential chimera sequences were removed. Eventually, the distribution of all OTUs was output as a $n \times m$ matrix where n is the number of OTUs and m is the number of samples.

1.5.6 OTUs filtering and phylotype assignment. Based on the OTU dataset, if an OTU appeared in only one among a total of 12 samples for each CO_2 condition, it was removed. This stringent OTU filtering criterion was to reduce noises (e.g., sequencing error, chimera and random sampling) of pyrosequence data, resulting in 3500 OTUs for further analysis. Finally, the longest sequences of each OTU were selected to assign a taxonomy by the RDP classifier (57). The confidence cutoff was set to 0.5.

1.5.7 Species richness, rarefaction and diversity calculations. The OTU numbers which were classified within a 0.03 distance were counted at different taxonomic (phylum, class, order, family or genus) levels for each sample or each CO_2 condition as the species richness. Also, the

estimated species richness was calculated by Chao's estimation method according to the rare species in each sample (34, 54), and the rarefaction method (40) was used to compare the species richness from two CO_2 conditions. Both calculations were carried out by the Mothur program (54). In addition, the Shannon index (43), also called as Shannon-Weaver index, was used to measure the diversity of each sample or each CO_2 condition. It was performed by the Vegan package (v.1.15-1) in R program (51), and principal coordinates analysis (PCoA) integrating the phylogenies of pyrosequencing data was performed by Fast UniFarc program (41) which was a phylogenetic-based β-diversity measurement.

1.5.8 Relative abundance calculation. Since the sequence numbers for individual samples were different, in order to compare the difference between both CO_2 conditions, we standardized the OTU distribution matrix into the relative abundance (RA) based on the following equation:

$$RA_{ij} = \frac{S_{ij}}{\sum_{j=1}^{n} S_{ij}} \times \underset{i=1}{\overset{m}{Max}}\left(\sum_{j=1}^{n} S_{ij}\right)$$

where i is the ith sample (1 to m), j is the jth OTU (1 to n) and S_{ij} is the number of sequences in ith sample and jth OTU. $\sum_{j=1}^{n} S_{ij}$ is the sum of sequences in ith sample and $\underset{i=1}{\overset{m}{Max}}\left(\sum_{j=1}^{n} S_{ij}\right)$ is the maximal number of total reads in all samples. Here m equals to 24 samples and n equals 3500 OTUs. All following statistical analyses were calculated based on this RA matrix.

1.6. Statistical analysis

1.6.1 Response ratio calculation. The effects of elevated CO_2 on phylogenetic composition and structure of microbial communities were analyzed by computing the response ratio (RR) using

the formula described by Luo et al. (47). Briefly, the mean and standard deviation (SD) of each treatment were extracted. The RR of each variable was calculated by dividing the mean of the treatment group to that of the control group. The variances for all comparisons were estimated by the means, the standard deviations, and the sample sizes in treatment and control groups, which were used to calculate the standard errors for each RR. Based on the standard error, the 95% confident interval for each response variable was obtained and the statistical difference between the elevated and ambient CO_2 conditions was estimated. For the response ratio analysis, the total relative abundance of each taxonomic level (phylum, class, order, family, or genus) was the sum of the relative abundance for all OTUs involving in this level.

1.6.2 Multivariate and direct gradient analysis. In this study, three different non-parametric analyses for multivariate data were used to examine whether eCO_2 has significant effects on soil microbial communities. These methods included analysis of similarities (ANOSIM) (35), non-parametric multivariate analysis of variance (adonis) using distance matrices (30), and multi-response permutation procedure (MRPP) (49). All three methods are based on Bray-Cutis dissimilarities among samples and their rank order in different ways to calculate test statistics, and the Monte Carlo permutation is used to test the significance of statistics. These three procedures were performed with the Vegan package (v.1.15-1) (39) in R project (51).

We also evaluated the correlations between the microbial population and soil or/and plant variables, to elucidate the inter-relationships among plant, soil, and microbial community. They were normalized to average 0 and standard deviation 1 before all other statistical analyses. First, all soil variables or plant variables were included in the Mantel test. They were virtually meaningless due to the noise and redundancy among those variables for soil or plant. Second, the BioENV procedure (36) was used to select the most correlated variables. The Bio-Env procedure

selected four soil variables, including the proportion of soil moisture at the depth of 0-17 cm (PSM0-17), %C at the depth of 0-10 cm (C0-10), %N at the depth of 0-10 cm (N0-10), and net N mineralization, and four plant variables, including belowground carbon % (BPC), aboveground carbon % (APC), aboveground total biomass (ATB), and total biomass (TB). To control possible co-varying effects between soil and plant variables, the partial Mantel test was performed. For the Mantel test, Euclidean distance was used to construct both dissimilarity matrices of communities and environmental variables respectively. All the analyses were performed by functions in the Vegan package (v.1.15-1) (39) in R v. 2.8.1 (51).

1.7. Phylogenetic analysis

A representative sequence was selected from each of 3500 OTUs, which was the longest sequence among all members for each OTU. Those 3500 sequences were aligned by PyNAST (32) with QIIME (33) integrated core 16S aligned sequences from Greengenes (38). The aligned sequences were used to construct the Neighbor-Joining tree with 500 times of bootstraps by using MEGA5 (44). Finally, the unrooted circle tree was visualized through the iTOL online program (45).

B. SUPPORTING TABLES

Table S1 Samples and their tagged primers used for amplifying 16S rRNA genes.

Sample	Tag	Tag seq.	16SForwardprimersequence (F515)	16Sreverseprimersequence (R907)
a67	C075	CGCAGA	CGAAGAGTGCCAGC**M**GCCGCGG	CGCAGACCGTCAATTC**M**TTT**R**AGTTT
a69	C077	CGCAGT	CGCAGTGTGCCAGC**M**GCCGCGG	CGCAGTCCGTCAATTC**M**TTT**R**AGTTT
a104	C079	CGCATG	CGCATGGTGCCAGC**M**GCCGCGG	CGCATGCCGTCAATTC**M**TTT**R**AGTTT
a107	C081	CGCGAT	CGCGATGTGCCAGC**M**GCCGCGG	CGCGATCCGTCAATTC**M**TTT**R**AGTTT
a184	C086	CGCTGA	CGCTGAGTGCCAGC**M**GCCGCGG	CGCTGACCGTCAATTC**M**TTT**R**AGTTT
a188	C083	CGCGTC	CGCGTCGTGCCAGC**M**GCCGCGG	CGCGTCCCGTCAATTC**M**TTT**R**AGTTT
a201	C084	CGCTAC	CGCTACGTGCCAGC**M**GCCGCGG	CGCTACCCGTCAATTC**M**TTT**R**AGTTT
a222	C094	CGTCGA	CGTCGAGTGCCAGC**M**GCCGCGG	CGTCGACCGTCAATTC**M**TTT**R**AGTTT
a306	C130	CTCGAG	CTCGAGGTGCCAGC**M**GCCGCGG	CTCGAGCCGTCAATTC**M**TTT**R**AGTTT
a344	C156	CTGCTG	CTGCTGGTGCCAGC**M**GCCGCGG	CTGCTGCCGTCAATTC**M**TTT**R**AGTTT
a355	C157	CTGTAC	CTGTACGTGCCAGC**M**GCCGCGG	CTGTACCCGTCAATTC**M**TTT**R**AGTTT
a358	C160	CTGTCG	CTGTCGGTGCCAGC**M**GCCGCGG	CTGTCGCCGTCAATTC**M**TTT**R**AGTTT
e23	C125	CTCAGT	CTCAGTGTGCCAGC**M**GCCGCGG	CTCAGTCCGTCAATTC**M**TTT**R**AGTTT
e33	C126	CTCATA	CTCATAGTGCCAGC**M**GCCGCGG	CTCATACCGTCAATTC**M**TTT**R**AGTTT
e45	C127	CTCATC	CTCATCGTGCCAGC**M**GCCGCGG	CTCATCCCGTCAATTC**M**TTT**R**AGTTT
e51	C128	CTCATG	CTCATGGTGCCAGC**M**GCCGCGG	CTCATGCCGTCAATTC**M**TTT**R**AGTTT
e147	C082	CGCGTA	CGCGTAGTGCCAGC**M**GCCGCGG	CGCGTACCGTCAATTC**M**TTT**R**AGTTT
e163	C088	CGCTGT	CGCTGTGTGCCAGC**M**GCCGCGG	CGCTGTCCGTCAATTC**M**TTT**R**AGTTT
e173	C089	CGTACG	CGTACGGTGCCAGC**M**GCCGCGG	CGTACGCCGTCAATTC**M**TTT**R**AGTTT
e179	C090	CGTAGC	CGTAGCGTGCCAGC**M**GCCGCGG	CGTAGCCCGTCAATTC**M**TTT**R**AGTTT
e250	C098	CGTCTG	CGTCTGGTGCCAGC**M**GCCGCGG	CGTCTGCCGTCAATTC**M**TTT**R**AGTTT
e270	C096	CGTCGT	CGTCGTGTGCCAGC**M**GCCGCGG	CGTCGTCCGTCAATTC**M**TTT**R**AGTTT
e272	C085	CGCTAG	CGCTAGGTGCCAGC**M**GCCGCGG	CGCTAGCCGTCAATTC**M**TTT**R**AGTTT
e283	C099	CGTGAC	CGTGACGTGCCAGC**M**GCCGCGG	CGTGACCCGTCAATTC**M**TTT**R**AGTTT

Table S2 Summary of numbers of sequences and OTUs, Chao and Shannon indices, and coverage for each sample at aCO_2 or eCO_2 based on pyrosequencing data.

Sample	No. of sequences	No. of OTUs (0.03)	Shannon Index
a104	2598	859	6.07
a107	3087	982	6.14
a184	2260	791	6.03
a188	2683	865	6.01
a201	2180	811	6.10
a222	2312	789	5.96
a306	2985	941	6.05
a344	1854	643	5.80
a355	2069	736	5.95
a358	2351	786	5.86
a67	2880	1012	6.23
a69	2749	946	6.24
aCO_2	**30008**	**2527**	**6.58**
e147	2854	883	6.07
e163	3299	919	5.97
e173	2119	752	5.96
e179	2584	820	5.97
e23	1810	665	5.92
e250	2547	779	5.97
e270	2845	931	6.14
e272	2821	952	6.22
e283	2690	931	6.18
e33	2065	702	5.81
e45	1759	619	5.66
e51	1698	653	5.88
eCO_2	**29091**	**2354**	**6.51**

Table S3. The classified phylotypes detected at different taxonomical levels.

	Domain	Phylum	Class	Order	Family	Genus
No. detected phylotypes	2	17	35	48	112	281
Shared at aCO_2 and eCO_2	2	16	31	39	96	213
Only detected at aCO_2	0	1	4	6	10	33
Only detected at eCO_2	0	0	0	3	6	35

Table S4. Statistical analysis of differences in the microbial community composition and structure between aCO_2 and eCO_2 at the community and phylum levels.

		MRPP[a]		anosim[b]		adonis[c]	
	No. OTUs	δ	*p*	R	*p*	R^2	*p*
All phylotypes	3500	0.481	**0.001**	0.209	**0.003**	0.082	**0.001**
Acidobacteria	369	0.478	**0.006**	0.157	**0.007**	0.078	**0.002**
Actinobacteria	596	0.370	**0.020**	0.132	**0.042**	0.086	**0.023**
Bacteroidetes	448	0.693	**0.001**	0.310	**0.001**	0.079	**0.001**
BRC1	2	0.935	0.102	0.048	0.958	0.000	1.000
Chlamydiae	36	0.936	**0.001**	0.198	**0.001**	0.000	1.000
Chloroflexi	94	0.620	0.099	0.043	0.142	0.067	0.163
Crenarchaeota	10	0.935	0.542	0.140	0.996	0.000	1.000
Cyanobacteria	3	0.641	0.061	0.103	**0.038**	0.069	0.059
Firmicutes	118	0.531	**0.002**	0.204	**0.002**	0.099	**0.002**
Gemmatimonadetes	86	0.538	0.057	0.091	0.058	0.088	0.101
Nitrospira	6	0.944	**0.005**	0.309	1.000	0.000	1.000
OP10	8	0.760	**0.001**	0.404	**0.001**	0.110	**0.001**
Planctomycetes	251	0.458	**0.023**	0.078	0.050	0.061	**0.018**
Proteobacteria	811	0.889	**0.003**	0.213	**0.002**	0.083	**0.002**
TM7	52	0.554	**0.012**	0.117	**0.024**	0.108	**0.008**
Verrucomicrobia	127	0.852	0.125	0.026	0.142	0.000	1.000
WS3	6	0.481	**0.001**	0.209	**0.003**	0.082	**0.001**

[a]MPRR: Multiple Response Permutation Procedure (49)

[b]anosim: Analysis of similarities (35)

[c]adonis: Analysis of variance using distance martrices (30)

Table S5. Numbers of shared OTUs that were significantly ($p < 0.05$) changed at eCO_2 based on the scaled abundances and unique OTUs detected only at aCO_2 or eCO_2.

Domain	Phylum	Shared OTUs		Unique OTUs	
		Down-eCO_2[a]	Up-eCO_2[b]	aCO_2	eCO_2
Archaea	Crenarchaeota	0	0	3	1
	Unclassified	0	0	1	0
Bacteria	Acidobacteria	5	2	134	68
	Actinobacteria	7	19	170	150
	Bacteroidetes	3	1	128	117
	BRC1	0	0	1	1
	Chlamydiae	0	0	14	19
	Chloroflexi	0	0	35	24
	Cyanobacteria	0	0	2	0
	Firmicutes	2	0	41	32
	Gemmatimonadetes	3	0	33	19
	Nitrospirae	0	0	2	0
	OP10	0	0	8	0
	Planctomycetes	1	2	99	79
	Proteobacteria	2	9	213	243
	TM7	0	0	22	17
	Verrucomicrobia	4	0	49	34
	WS3	0	0	2	3
	Unclassified	0	2	184	158
Unclassified		0	1	5	8
Total		27	36	1146	973

a: Down-eCO_2 means the shared OTUs were significantly lower in eCO_2 samples than aCO_2 samples by unpaired Stundent T tests.

b: Up-eCO_2 means the shared OTUs were significantly higher in eCO_2 samples than aCO_2 samples by unpaired Student t tests.

Table S6. Partial Mantel analysis of the relationship between the relative abundance of phylum and soil or plant properties. Selected soil and plant variables are described in Table 2.

		Soil[a]		Plant[b]	
In association with: controlling		Plant[b]		Soil[a]	
Domain	Phylum	r	p	r	p
All detected OTUs		-0.018	0.508	0.266	0.065
Archaea	Crenarchaeota	-0.145	0.829	0.074	0.269
Bacteria	Acidobacteria	-0.027	0.560	-0.045	0.582
	Actinobacteria	0.000	0.396	0.137	0.112
	BRC1	-0.248	0.977	0.107	0.229
	Bacteroidetes	0.173	0.164	0.152	0.127
	Firmicutes	0.190	0.122	0.357	**0.027**
	OP10	0.057	0.281	-0.172	0.921
	Planctomycetes	0.234	0.113	-0.023	0.488
	Proteobacteria	0.170	0.155	0.414	**0.014**
	TM7	-0.026	0.549	0.002	0.459
	Chlamydiae	-0.037	0.517	0.406	**0.008**
	Chloroflexi	-0.004	0.411	-0.160	0.889
	Cyanobacteria	0.050	0.374	0.097	0.282
	Gemmatimonadetes	0.246	0.055	0.480	**0.000**
	Nitrospirae	-0.066	0.594	0.416	**0.018**
	Verrucomicrobia	-0.185	0.940	0.091	0.183
	WS3	-0.122	0.847	-0.085	0.761

Table S7. Partial Mantel analysis of the relationship between the relative abundance of order and soil or plant properties. Only significantly ($p < 0.05$) correlated phylotypes are shown. Selected soil and plant variables are listed in Table 2.

			Soil		Plant	
In association with: controlling			Plant		Soil	
Phylum	Class	Order	r	p	r	p
Firmicutes	Bacilli	Bacillales	0.180	0.133	0.381	**0.022**
	Clostridia	Clostridiales	0.335	**0.049**	0.552	**0.008**
Proteobacteria	α-Proteobacteria	Caulobacterales	-0.125	0.799	0.295	**0.039**
		Rhizobiales	0.170	0.087	0.284	**0.006**
	β-Proteobacteria	Burkholderiales	0.243	0.075	0.468	**0.003**
		Chromatiales	0.242	**0.032**	-0.071	0.712
		Legionellales	0.214	0.120	0.373	**0.030**
		Pseudomonadales	0.257	0.057	0.318	**0.041**
		Thiotrichales	0.095	0.278	0.519	**0.006**
TM7	Unclassified	Unclassified	-0.066	0.596	0.416	**0.019**
Chlamydiae	Chlamydiae	Chlamydiales	0.190	0.136	0.357	**0.030**
Nitrospirae	Nitrospira	Nitrospirales	-0.037	0.516	0.406	**0.010**

Table S8. Partial Mantel analysis of the relationship between the relative abundance of family and soil or plant properties. Only significantly ($p < 0.05$) changed phytotypes are shown, and selected soil and plant variables are listed in Table 2.

				Soil		Plant	
In association with: controlling				Plant		Soil	
Phylum	Class	Order	Family	*r*	*p*	*r*	*p*
Actinobacteria	Actinobacteria	Actinomycetales	Microbacteriaceae	-0.198	0.983	0.185	**0.047**
			Thermomonosporaceae	0.254	**0.044**	-0.202	0.979
Chlamydiae	Chlamydiae	Chlamydiales	Parachlamydiaceae	0.177	0.151	0.355	**0.022**
Firmicutes	Bacilli	Bacillales	Bacillaceae	0.206	0.116	0.414	**0.015**
			Paenibacillaceae	0.155	0.184	0.360	**0.038**
			Planococcaceae	0.075	0.270	0.274	**0.035**
	Clostridia	Clostridiales	Clostridiaceae	0.421	**0.015**	0.553	**0.003**
Nitrospirae	Nitrospirae	Nitrospirales	Nitrospiraceae	-0.037	0.580	0.406	**0.008**
Proteobacteria	α-Proteobacteria	Caulobacterales	Caulobacteraceae	-0.125	0.793	0.299	**0.040**
		Rhizobiales	Aurantimonadaceae	0.357	**0.031**	0.098	0.188
			Beijerinckiaceae	0.138	0.216	0.297	**0.033**
			Bradyrhizobiaceae	0.207	**0.046**	0.232	**0.030**
			Rhodobiaceae	0.129	0.148	0.397	**0.023**
		Rhodospirillales	Rhodospirillaceae	-0.162	0.865	0.472	**0.004**
		Unclassified	Alphaproteobacteria incertae sedis	0.106	0.262	0.360	**0.012**
	β-Proteobacteria	Burkholderiales	Burkholderiaceae	0.416	**0.019**	0.377	**0.034**
			Burkholderiales incertae sedis	-0.183	0.938	0.371	**0.009**
			Oxalobacteraceae	0.254	**0.035**	0.372	**0.009**
	γ-Proteobacteria	Chromatiales	Chromatiaceae	0.500	**0.001**	-0.267	0.991
		Legionellales	Coxiellaceae	0.171	0.147	0.426	**0.016**
		Pseudomonadales	Pseudomonadaceae	0.262	0.059	0.320	**0.033**
		Thiotrichales	Unclassified	0.095	0.292	0.519	**0.008**
TM7	Unclassified	Unclassified	Unclassified	-0.066	0.575	0.416	**0.019**

Table S9 Partial Mantel analysis of the relationship between the relative abundance of genus and soil or plant properties. Only significantly ($p < 0.05$) changed phytotypes are shown, and selected soil and plant variables are listed in Table 2.

					Soil		Plant	
In association with: controlling					Plant		Soil	
Phylum	Class	Order	Family	Genus	r	p	r	p
Actinobacteria	Actinobacteria	Actinomycetales	Microbacteriaceae	Microbacterium	-0.050	0.585	0.422	0.002
				Plantibacter	-0.058	0.590	0.401	0.003
				Unclassified	-0.008	0.504	0.301	0.007
			Nocardiaceae	Rhodococcus	0.270	0.078	-0.088	0.693
			Nocardioidaceae	Actinopolymorpha	0.173	0.151	0.461	0.034
				Marmoricola	0.284	0.050	-0.146	0.874
			Propionibacteriaceae	Micropruina	0.528	0.009	-0.294	0.996
			Thermomonosporaceae	Actinoallomurus	0.267	0.042	-0.192	0.977
Bacteroidetes	Flavobacteria	Flavobacteriales	Cryomorphaceae	Fluviicola	0.116	0.224	0.504	0.011
	Sphingobacteria	Sphingobacteriales	Chitinophagaceae	Flavisolibacter	0.171	0.124	0.374	0.004
				Terrimonas	0.115	0.247	0.414	0.017
			Cytophagaceae	Sporocytophaga	0.344	0.026	-0.172	0.942
			Sphingobacteriaceae	Solitalea	0.382	0.010	0.006	0.424
Chlamydiae	Chlamydiae	Chlamydiales	Parachlamydiaceae	Parachlamydia	0.143	0.202	0.368	0.018
Firmicutes	Bacilli	Bacillales	Bacillaceae	Tumebacillus	0.334	0.084	0.594	0.007
				Unclassified	0.028	0.415	0.316	0.026
			Bacillales	incertae	0.156	0.218	0.357	0.037
			Paenibacillaceae	Ammoniphilus	0.287	0.063	0.372	0.029
				Paenibacillus	0.146	0.223	0.360	0.046
			Planococcaceae	Sporosarcina	0.076	0.228	0.275	0.036
	Clostridia	Clostridiales	Clostridiaceae	Clostridium	0.421	0.012	0.553	0.006
Nitrospirae	Nitrospirae	Nitrospirales	Nitrospiraceae	Nitrospira	-0.037	0.539	0.406	0.006
Planctomycetes	Planctomycetacia	Planctomycetales	Planctomycetaceae	Gemmata	-0.109	0.754	0.371	0.017
Proteobacteria	α-Proteobacteria	Caulobacterales	Caulobacteraceae	Phenylobacterium	-0.130	0.820	0.372	0.036
		Rhizobiales	Aurantimonadaceae	Aurantimonas	0.357	0.025	0.098	0.203
			Beijerinckiaceae	Chelatococcus	0.278	0.065	0.462	0.012
			Bradyrhizobiaceae	Bradyrhizobium	0.199	0.054	0.228	0.034
				Rhodopseudomonas	0.261	0.016	0.032	0.327
			Brucellaceae	Ochrobactrum	0.376	0.033	0.367	0.055
			Methylobacteriaceae	Unclassified	0.215	0.047	-0.124	0.825
			Rhodobiaceae	Anderseniella	0.146	0.145	0.375	0.013
		Rhodospirillales	Acetobacteraceae	Roseomonas	0.202	0.077	-0.052	0.635
			Rhodospirillaceae	Skermanella	-0.294	1.000	0.333	0.042
				Thalassobaculum	0.288	0.056	-0.200	0.971
				Unclassified	0.061	0.314	0.270	0.043
		Sphingomonadales	Erythrobacteraceae	Unclassified	-0.254	0.979	0.191	0.098
			Sphingomonadaceae	Unclassified	-0.028	0.488	0.317	0.038
		Unclassified	Unclassified	incertae	0.106	0.257	0.360	0.021
	β-Proteobacteria	Burkholderiales	Burkholderiaceae	Burkholderia	0.437	0.016	0.365	0.044
				Ralstonia	0.019	0.400	0.321	0.025
			Burkholderiales	incertae sedis	0.230	0.115	0.360	0.033
				incertae sedis	-0.188	0.955	0.431	0.007
			Comamonadaceae	Unclassified	-0.028	0.468	0.409	0.047
			Oxalobacteraceae	Herminiimonas	0.361	0.050	-0.135	0.897
				Massilia	0.176	0.110	0.376	0.021
	δ-Proteobacteria	Myxococcales	Polyangiaceae	Unclassified	0.319	0.046	0.106	0.221
	γ-Proteobacteria	Chromatiales	Chromatiaceae	Nitrosococcus	0.500	0.000	-0.267	0.995
		Legionellales	Coxiellaceae	Aquicella	0.171	0.140	0.426	0.006
			Legionellaceae	Unclassified	0.321	0.058	0.447	0.021
		Pseudomonadales	Pseudomonadaceae	Pseudomonas	0.266	0.064	0.317	0.040
		Thiotrichales	Unclassified	Unclassified	0.095	0.272	0.519	0.011
		Xanthomonadales	Xanthomonadaceae	Lysobacter	-0.038	0.510	0.268	0.063
TM7	Unclassified	Unclassified	Unclassified	TM7	-0.066	0.598	0.416	0.017
Verrucomicrobia	Subdivision3	Unclassified	Unclassified	Subdivision3 genera	0.285	0.038	-0.190	0.908

D. SUPPORTING FIGURES

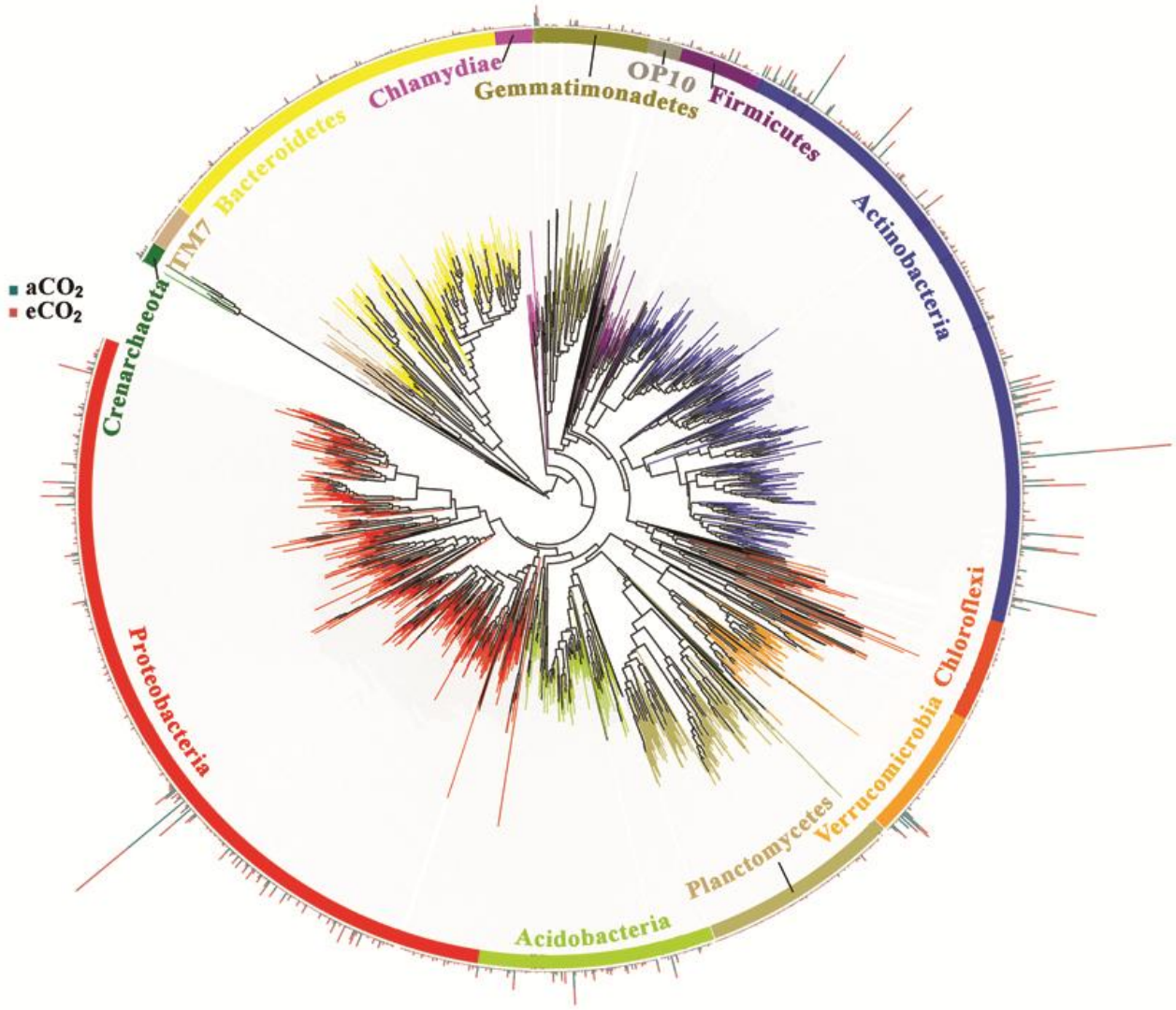

Fig. S1. Neighbor-Joining tree of representative sequences of 16S rRNA genes major phyla detected at aCO_2 and eCO_2. Different phyla are presented by different colors on the circle tree. The relative abundance of each OTU is indicated on the periphery of the circle tree by the color bar with blue for aCO_2 and red for eCO_2 samples, which is proportion to the bar height. All unclassified OTUs (13.6%) at the phylum level were excluded from tree construction. Also, four phyla (BRC1, Cynobacteria, WS3 and Nitroapirae) with six or fewer OTUs detected are not shown in this tree.

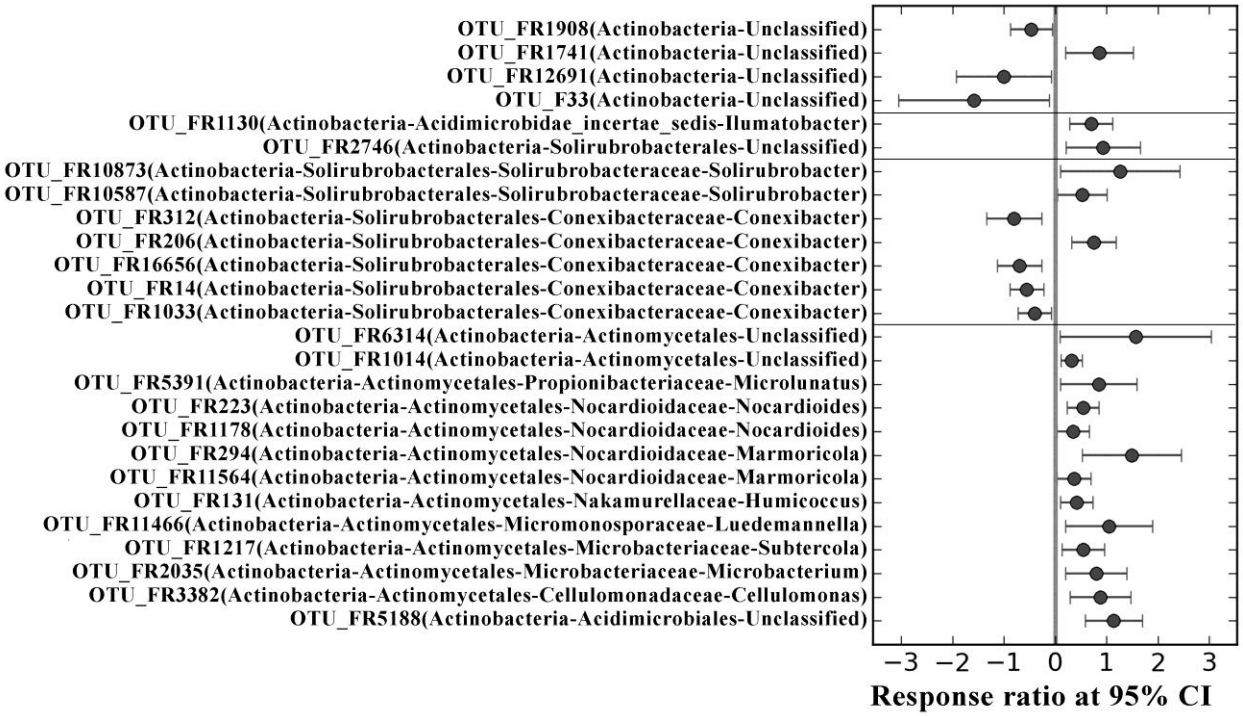

Fig. S2 Significantly changed OTUs in the phylum of Actinobacteria at elevated CO_2 using the response ratio method (47) at 95% confidence interval.

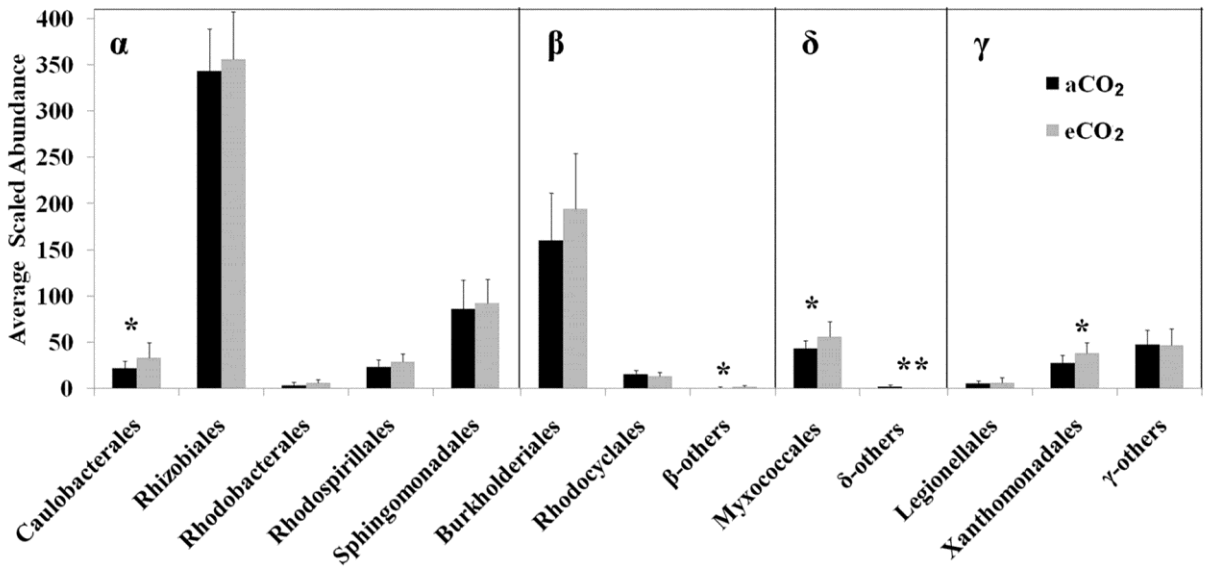

Fig. S3. Significantly changed microbial populations at the order levels in the phylum of Proteobacteria. Significance was tested by response ratios (47). *: $p < 0.05$; **: $p < 0.01$.

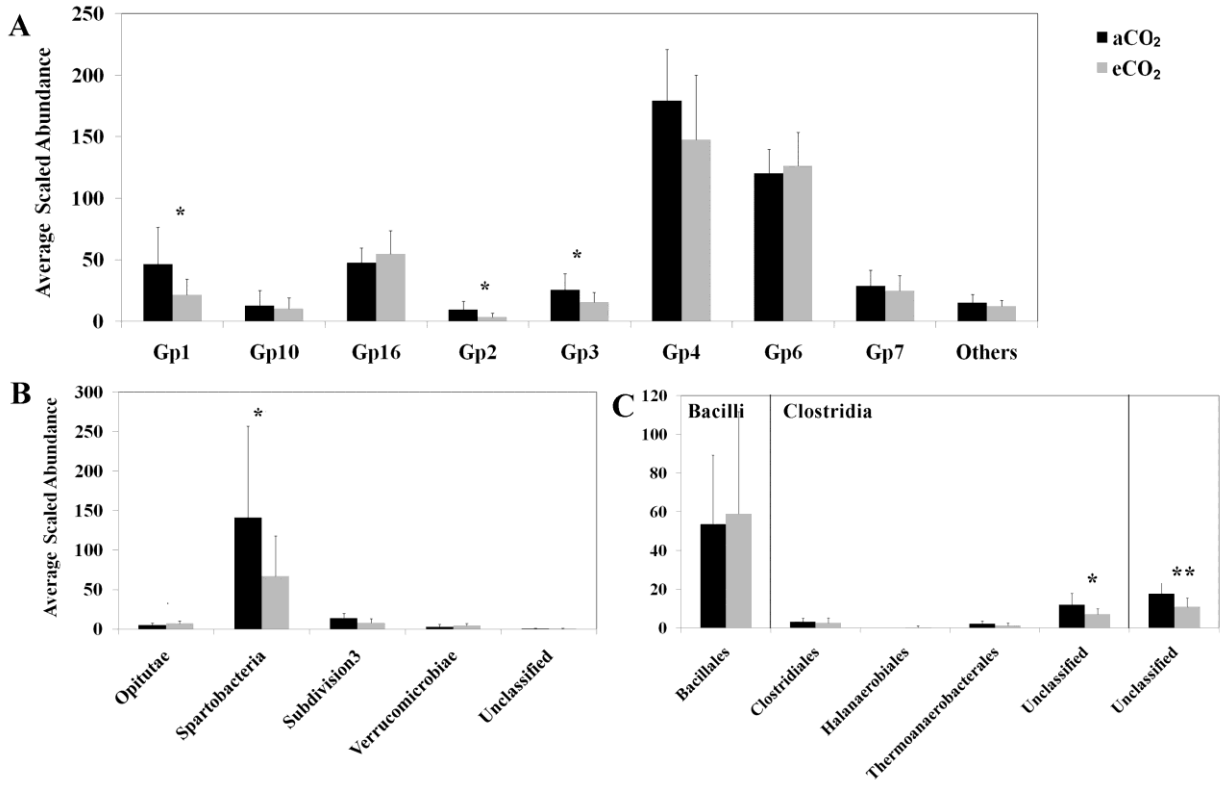

Fig. S4. Significantly changed microbial populations at the class or lower levels in the phylum of Acidobacteria (A), Verrucomicrobia (B), and Firmicutes (C). Significance was tested by response ratios (47). *: $p < 0.05$; **: $p < 0.01$.

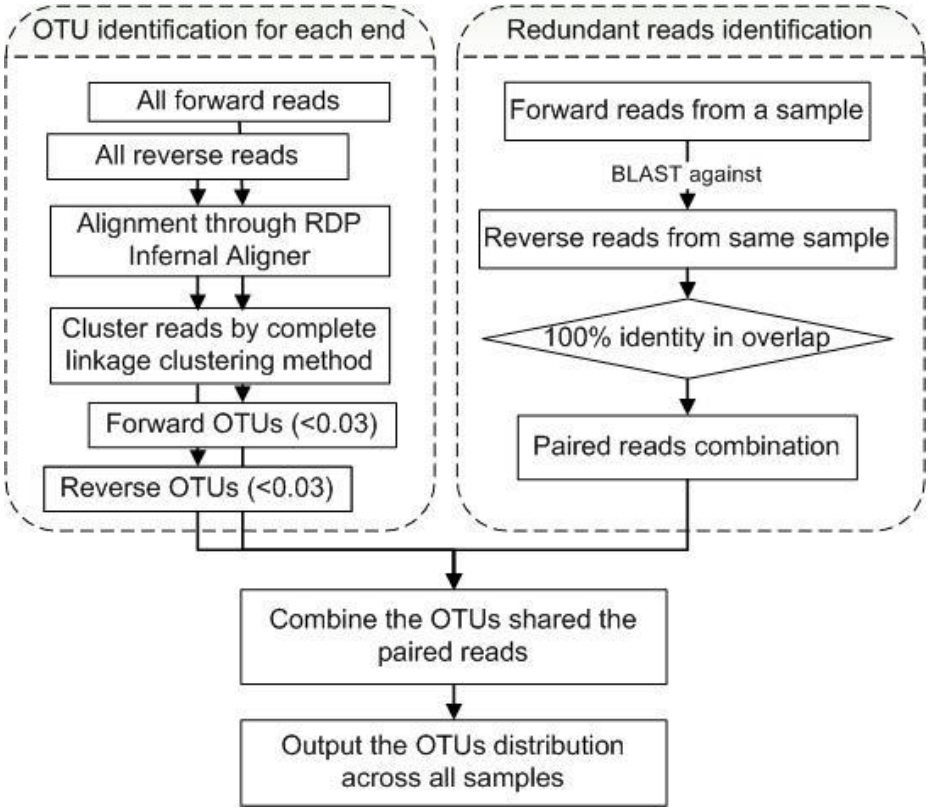

Fig. S5 The flowchart of OTU identification processes.

SUPPLEMENTAL REFERENCES

29. **Ahn, S., J. Costa, and J. Emanuel.** 1996. PicoGreen quantitation of DNA: effective evaluation of samples pre- or post-PCR. Nucl. Acids Res. **24:**2623-2625.

30. **Anderson, M. J.** 2001. A new method for non-parametric multivariate analysis of variance. Austral Ecol **26:**32-46.

31. **Binladen, J., M. T. Gilbert, J. P. Bollback, F. Panitz, C. Bendixen, R. Nielsen, and E. Willerslev.** 2007. The use of coded PCR primers enables high-throughput sequencing of multiple homolog amplification products by 454 parallel sequencing. PLoS ONE **2:**e197.

32. **Caporaso, J. G., K. Bittinger, F. D. Bushman, T. Z. DeSantis, G. L. Andersen, and R. Knight.** 2010. PyNAST: a flexible tool for aligning sequences to a template alignment. Bioinformatics **26:**266-267.

33. **Caporaso, J. G., J. Kuczynski, J. Stombaugh, K. Bittinger, F. D. Bushman, E. K. Costello, N. Fierer, A. G. Pena, J. K. Goodrich, J. I. Gordon, G. A. Huttley, S. T. Kelley, D. Knights, J. E. Koenig, R. E. Ley, C. A. Lozupone, D. McDonald, B. D. Muegge, M. Pirrung, J. Reeder, J. R. Sevinsky, P. J. Turnbaugh, W. A. Walters, J. Widmann, T. Yatsunenko, J. Zaneveld, and R. Knight.** 2010. QIIME allows analysis of high-throughput community sequencing data. Nat Methods **7:**335-336.

34. **Chao, A.** 1987. Estimating the population size for capture-recapture data with unequal catchability. Biometrics **43:**783-791.

35. **Clarke, K. R.** 1993. Nonparametric Multivariate Analyses of Changes in Community Structure. Aust J Ecol **18:**117-143.

36. **Clarke, K. R., and M. Ainsworth.** 1993. A Method of Linking Multivariate Community Structure to Environmental Variables. Mar Ecol-Prog Ser **92:**205-219.

37. **Cole, J. R., Q. Wang, E. Cardenas, J. Fish, B. Chai, R. J. Farris, A. S. Kulam-Syed-Mohideen, D. M. McGarrell, T. Marsh, G. M. Garrity, and J. M. Tiedje.** 2009. The Ribosomal Database Project: improved alignments and new tools for rRNA analysis. Nucleic Acids Res **37:**D141-145.

38. **DeSantis, T. Z., P. Hugenholtz, N. Larsen, M. Rojas, E. L. Brodie, K. Keller, T. Huber, D. Dalevi, P. Hu, and G. L. Andersen.** 2006. Greengenes, a chimera-checked

16S rRNA gene database and workbench compatible with ARB. Appl Environ Microbiol **72:**5069-5072.

39. **Dixon, P.** 2003. VEGAN, a package of R functions for community ecology. J. Veg. Sci. **14:**927-930.

40. **Gotelli, N. J., and R. K. Colwell.** 2001. Quantifying biodiversity: procedures and pitfalls in the measurement and comparison of species richness. Ecol. Lett. **4:**379-391.

41. **Hamady, M., C. Lozupone, and R. Knight.** 2010. Fast UniFrac: facilitating high-throughput phylogenetic analyses of microbial communities including analysis of pyrosequencing and PhyloChip data. ISME J. **4:**17-27.

42. **Hamady, M., J. J. Walker, J. K. Harris, N. J. Gold, and R. Knight.** 2008. Error-correcting barcoded primers for pyrosequencing hundreds of samples in multiplex. Nat. Methods **5:**235-237.

43. **Krebs, C. J.** 1989. Ecological methodology. Harper & Row, New York.

44. **Kumar, S., M. Nei, J. Dudley, and K. Tamura.** 2008. MEGA: a biologist-centric software for evolutionary analysis of DNA and protein sequences. Brief Bioinform **9:**299-306.

45. **Letunic, I., and P. Bork.** 2007. Interactive Tree Of Life (iTOL): an online tool for phylogenetic tree display and annotation. Bioinformatics **23:**127-128.

46. **Lewin, G. R., E. Mckintosh, and S. B. Mcmahon.** 1994. Nmda Receptors and Activity-Dependent Tuning of the Receptive-Fields of Spinal-Cord Neurons. Nature **369:**482-485.

47. **Luo, Y. Q., D. F. Hui, and D. Q. Zhang.** 2006. Elevated CO2 stimulates net accumulations of carbon and nitrogen in land ecosystems: A meta-analysis. Ecology **87:**53-63.

48. **Margulies, M., M. Egholm, W. E. Altman, S. Attiya, J. S. Bader, L. A. Bemben, J. Berka, M. S. Braverman, Y. J. Chen, Z. Chen, S. B. Dewell, L. Du, J. M. Fierro, X. V. Gomes, B. C. Godwin, W. He, S. Helgesen, C. H. Ho, G. P. Irzyk, S. C. Jando, M. L. Alenquer, T. P. Jarvie, K. B. Jirage, J. B. Kim, J. R. Knight, J. R. Lanza, J. H. Leamon, S. M. Lefkowitz, M. Lei, J. Li, K. L. Lohman, H. Lu, V. B. Makhijani, K. E. McDade, M. P. McKenna, E. W. Myers, E. Nickerson, J. R. Nobile, R. Plant, B. P. Puc, M. T. Ronan, G. T. Roth, G. J. Sarkis, J. F. Simons, J. W. Simpson, M.**

Srinivasan, K. R. Tartaro, A. Tomasz, K. A. Vogt, G. A. Volkmer, S. H. Wang, Y. Wang, M. P. Weiner, P. Yu, R. F. Begley, and J. M. Rothberg. 2005. Genome sequencing in microfabricated high-density picolitre reactors. Nature **437:**376-380.

49. **Mielke, P. W., K. J. Berry, P. J. Brockwell, and J. S. Williams.** 1981. A Class of Nonparametric-Tests Based on Multiresponse Permutation Procedures. Biometrika **68:**720-724.

50. **Nawrocki, E. P., and S. R. Eddy.** 2007. Query-dependent banding (QDB) for faster RNA similarity searches. PLoS Comput Biol **3:**e56.

51. **R Development Core Team** 2010, posting date. R: A Language and Environment for Statistical Computing. [Online.]

52. **Reich, P. B., S. E. Hobbie, T. Lee, D. S. Ellsworth, J. B. West, D. Tilman, J. M. Knops, S. Naeem, and J. Trost.** 2006. Nitrogen limitation constrains sustainability of ecosystem response to CO2. Nature **440:**922-925.

53. **Reich, P. B., J. Knops, D. Tilman, J. Craine, D. Ellsworth, M. Tjoelker, T. Lee, D. Wedin, S. Naeem, D. Bahauddin, G. Hendrey, S. Jose, K. Wrage, J. Goth, and W. Bengston.** 2001. Plant diversity enhances ecosystem responses to elevated CO2 and nitrogen deposition. Nature **410:**809-812.

54. **Schloss, P. D., S. L. Westcott, T. Ryabin, J. R. Hall, M. Hartmann, E. B. Hollister, R. A. Lesniewski, B. B. Oakley, D. H. Parks, C. J. Robinson, J. W. Sahl, B. Stres, G. G. Thallinger, D. J. Van Horn, and C. F. Weber.** 2009. Introducing mothur: open-source, platform-independent, community-supported software for describing and comparing microbial communities. Appl. Environ. Microbiol. **75:**7537-7541.

55. **Stackebrandt, E., and B. M. Goebel.** 1994. Taxonomic Note: A Place for DNA-DNA Reassociation and 16S rRNA Sequence Analysis in the Present Species Definition in Bacteriology. Int J Syst Bacteriol **44:**846-849.

56. **Sun, Y., Y. Cai, L. Liu, F. Yu, M. L. Farrell, W. McKendree, and W. Farmerie.** 2009. ESPRIT: estimating species richness using large collections of 16S rRNA pyrosequences. Nucleic Acids Research **37:**e76.

57. **Wang, Q., G. M. Garrity, J. M. Tiedje, and J. R. Cole.** 2007. Naive Bayesian classifier for rapid assignment of rRNA sequences into the new bacterial taxonomy. Appl Environ Microbiol **73:**5261-5267.

58. **Zhou, J. Z., M. A. Bruns, and J. M. Tiedje.** 1996. DNA recovery from soils of diverse composition. Appl. Environ. Microbiol. **62:**316-322.